

# Interpretation of multi-TeV photons from GRB221009A

Ali Baktash,<sup>1</sup> Dieter Horns<sup>1</sup> and Manuel Meyer<sup>2</sup>

Universität Hamburg, Luruper Chaussee 149, D-22761 Hamburg, Germany

E-mail: [ali.baktash@uni-hamburg.de](mailto:ali.baktash@uni-hamburg.de), [dieter.horns@uni-hamburg.de](mailto:dieter.horns@uni-hamburg.de),  
[manuel.meyer@uni-hamburg.de](mailto:manuel.meyer@uni-hamburg.de)

**Abstract.** The nearby GRB221009A at redshift  $z = 0.1505$  has been observed up to a maximum energy of 18 TeV with the LHAASO air shower array. The expected optical depth for a photon with energy  $E_\gamma = 18$  TeV varies between 9.4 and 27.1 according to existing models of the extra-galactic background light (EBL) in the relevant mid infra-red range. The resulting suppression of the flux in several EBL models makes it unlikely that this photon could have been observed at the claimed energy. If the photon event and its energy are confirmed and possibly even more photons above 10 TeV have been observed, the photon-pair production process would have to be suppressed by mechanisms predicted in extensions of the Standard Model of particle physics. We consider the possibilities of photon mixing with a light pseudo-scalar (e.g., axion-like particles; ALPs) in the magnetic field of the host galaxy and the Milky Way and Lorentz invariance violation (LIV). In the case of photon-ALP mixing, the boost factor would reach values  $\sim 10^6$  for photon couplings not ruled out by the CAST experiment, but limited by other astrophysical constraints. Viable scenarios would require either very efficient mixing in or near to the GRB or that the largest part of the total luminosity is radiated at TeV energies, different from previous GRB afterglows. In the case of LIV, required boost factors are achievable for a LIV breaking energy scale  $\lesssim 2 \times 10^{29}$  eV ( $\lesssim 4 \times 10^{21}$  eV) for the linear (quadratic) modification of the dispersion relation. A more simple explanation would be a misidentification of a charged cosmic-ray air shower.

**Keywords:** gamma-ray burst, extra-galactic background light, GRB221009A, Lorentz invariance violation, ALPs, axions

**ArXiv ePrint:** [2210.07172](https://arxiv.org/abs/2210.07172)

---

<sup>1</sup>Corresponding author.

<sup>2</sup>Now at CP3-Origins, University of Southern Denmark, Campusvej 55, DK-5230 Odense M, Denmark

---

## Contents

<b>1</b>	<b>Introduction</b>	<b>1</b>
<b>2</b>	<b>Origin of the 18 TeV photon</b>	<b>2</b>
2.1	Absorption in the extra-galactic background light	2
2.2	Expected photon and background counts	3
2.3	Reducing the gamma-ray opacity with Physics beyond the Standard Model	7
2.3.1	Photon mixing with light pseudo-scalar (axion-like) particle	7
2.3.2	Photon opacity in LIV scenarios	9
<b>3</b>	<b>Conclusions</b>	<b>11</b>

---

## 1 Introduction

The exceptionally bright GRB221009A was registered with the BAT instrument onboard the *Swift* satellite on 2022-10-09 at 14:10:17 UT. The object was subsequently detected with the XRT and the UVOT (reported in the Gamma-ray Coordinates Network Notice GCN 32632<sup>1</sup>). Given the exceptional brightness of the object and its proximity to the Galactic plane ( $l = 52^{\circ}57^m27.8^s$ ,  $b = 04^{\circ}19'17.9''$ ), the object was initially considered to be a Galactic X-ray transient (Swift J1913.1+1946). The earlier trigger at 13:16:59.00 UT (in the following  $t_0$ ) of the Gamma-ray burst monitor (GBM, GCN 32636) and the subsequent detection with the large-area telescope (LAT, GCN 32637) at 14:17:05.99 UT on board the *Fermi* satellite made clear that the object is the brightest gamma-ray burst event detected so far. The emission was sufficiently bright that photons were detected with the LAT  $\sim 25$  ksec after the burst occurred. The most energetic photon with  $E_{\gamma} = 99.3$  GeV (detected at  $t_0 + 240$  s) is the photon with the highest energy detected from any GRB with *Fermi* LAT<sup>2</sup> (GCN 32658). The energy spectrum above 100 MeV is characterised with a power law with photon index  $-1.87 \pm 0.04$  with an integrated flux between 100 MeV and 1 GeV of  $(6.2 \pm 0.4) \times 10^{-3} \text{ cm}^{-2} \text{ s}^{-1}$ . The quoted flux is averaged in the time interval from  $t_0 + 200$  s to  $t_0 + 800$ s. The temporal structure of the GBM light curve indicates that the first maximum was followed by a brighter emission period with multiple maxima with a duration  $t_{90} \approx 327$  s (GCN 32642). The fluence of the second maximum at  $0.03 \text{ erg/cm}^2$  is affected by saturation. The peak photon flux at  $t_0 + 238$  s is  $(2385 \pm 3) \text{ ph cm}^{-2} \text{ s}^{-1}$ .

Given the exceptional brightness at X-rays and high energy gamma rays, it is expected that the object is rather nearby. The first red-shift estimate obtained at  $t_0 + 11.55$  hrs from a spectrum taken with the X-shooter at VLT (GCN 32648) is based upon the detection of absorption lines (CaII, CaI) at  $z = 0.151$  ( $d_L = 753$  Mpc). This measurement is confirmed with the GTC (GCN 32686:  $z = 0.1505$ ) and provides an estimate of the isotropic energy release using the GBM fluence of  $2 \times 10^{54} \text{ erg} \approx 1M_{\odot}c^2$ . According to the preliminary classification of the object (GCN 32686), GRB221009A is a type II (collapsar) burst [1, 2] or a binary-driven hypernova (GCN 32780) [3].

---

<sup>1</sup>See <https://gcn.gsfc.nasa.gov/>

<sup>2</sup>the previous record holder was observed with  $E_{\gamma} = 95$  GeV from GRB130427A at  $z = 0.34$ .

## 2 Origin of the 18 TeV photon

The observational data obtained with various space-based X-ray and gamma-ray instruments will provide important information on the origin of the emission and the nature of the object. However, in the following, we will focus our analysis on the very high energy emission that was observed with the LHAASO experiment.<sup>3</sup> The LHAASO collaboration reported in GCN 32677 the detection of the GRB both with the water Cherenkov Detector Array (WCDA) (significance of  $100\sigma$ ) and the larger air shower detector KM2A (significance of  $10\sigma$ ) within  $t_0$  and  $t_0+2000$  s. The total number of photons above 500 GeV reported is  $\geq 5000$  reaching up to a maximum photon energy of 18 TeV. In the following, we assume the detection of the most energetic photon with KM2A which features a relative energy resolution of  $\sigma_E/E_\gamma \approx 40\%$  [6]. The object was observed at a zenith angle distance from  $30^\circ$  to  $35^\circ$ . In Fig. 1, the spectral energy distribution (SED) of GRB221009A as measured with *Fermi*-LAT is extra-polated to higher energies, where the observed flux is affected by photon-photon pair production on the extra-galactic background light. As a comparison, we have included in Fig. 1 the SED of the Crab Nebula in the same energy range [7]. The peak in the SED of GRB221009A is located beyond the energy range covered with *Fermi*-LAT. For a peak energy of  $\approx 100$  GeV, the extra-polated and time-average power received from GRB221009A from  $t_0 + 200$  s... 800 s is approximately a factor  $10^4$  larger than the power received from the Crab Nebula.

### 2.1 Absorption in the extra-galactic background light

The process of photon-photon pair-production ( $\gamma + \gamma \rightarrow e^+ + e^-$ ) has been known for a long time [8] to suppress the apparent brightness of gamma-rays with energies  $E_\gamma \gtrsim 100$  GeV.

The resulting optical depth  $\tau$  of a photon of observed energy  $E_\gamma$  relates closely to the number of photons per volume and energy interval present in the inter-galactic medium at wavelength  $\lambda$  with  $\lambda \approx 1.2 \mu\text{m}(E_\gamma/\text{TeV})$ . Since the EBL is difficult to detect against dominating foreground emission of the interplanetary and interstellar medium, the optical depth is calculated under the assumption of an underlying model for the EBL. Even though the various models and both direct and indirect estimates of the EBL have been converging in the past decades for the wavelength range close to the optical and near-infrared, the uncertainties at larger wavelengths remain substantial.

In Tab. 2.1, we list the optical depth values for a photon of nominal energy  $E_\gamma = 18$  TeV and  $E_\gamma - \sigma_E \approx 10$  TeV detected from a red shift  $z = 0.1505$  using a selection of models for the EBL.<sup>4</sup> For a given optical depth  $\tau$ , the observed flux is attenuated by a factor  $\exp(-\tau)$  which in this case ranges from  $\exp(-27.1) = 1.7 \times 10^{-12}$  for the upper bound model of Ref. [9] at  $E_\gamma = 18$  TeV to  $\exp(-4.5) = 10^{-3}$  for the lower bound model of Ref. [9] at  $E_\gamma = 10$  TeV. The photon density of the EBL in the mid infra-red at wave-lengths from  $\lambda = 5 \mu\text{m}$  to  $\lambda = 20 \mu\text{m}$  is most relevant for the estimated optical depth at gamma-ray energies above 10 TeV. The accuracy of the models suffer however from uncertainties on the amount of stellar light re-processed by polycyclic aromatic hydrocarbon (PAH) molecules present in the galaxies.

The effect of absorption leads to a strong suppression of the observable flux at TeV energies. In Fig. 1, we show for orientation the flux measurement of GRB221009A during the time-interval from  $t_0 + 200$  s to  $t_0 + 800$  s obtained with *Fermi* LAT (GCN 32658). The uncertainty on the flux and the photon index constrain a bow-tie shaped region in

---

<sup>3</sup>In this context, two other independent studies related to the optical depth [4] and violation of Lorentz invariance violation [5] have appeared as pre-prints

<sup>4</sup>We use the public repository of collected tables at <https://github.com/me-manu/ebhtable>.

**Table 1.** For a set of models for the extra-galactic background light (EBL; K&D2010: [10], Fi2010: [11], Gi2012(f): [12], Do2011( $\pm$ ): [9], Fr2008: [13], SL2021: [14]) we list the resulting optical depth values  $\tau$  for the nominal photon energy of 18 TeV ( $\tau_{18}$ ) and for a lower bound of 10 TeV ( $\tau_{10}$ ) within the range of a relative energy resolution of  $\approx 40\%$ . Expected number of photons for  $\zeta = 5$ ,  $t_1 = 200$  s, above 500 GeV (18 TeV):  $N_{\gamma,0.5}$  ( $N_{\gamma,18}$ ) and required coupling to ALPs  $g_{a\gamma}$  in units of  $10^{-11}$  GeV $^{-1}$ , as well as (maximum) energy for Lorentz invariance breaking ( $M_{1,2}$  for linear and quadratic modifications of the dispersion relation) in units of Planck mass  $M_{\text{Pl}} = (\hbar c^5/G)^{1/2} \approx 1.22 \times 10^{28}$  eV.

EBL Model	$\tau_{18}$	$\tau_{10}$	$N_{\gamma,0.5}$	$N_{\gamma,18}$	$g_{a\gamma}$	$M_1(M_2)$
K&D2010	9.4	4.5	6700	1	-	- (-)
Fi2010	10.0	6.0	4162	0.9	-	- (-)
Gi2012	13.3	5.4	4500	$2 \times 10^{-2}$	0.58	10.4 ( $2.6 \times 10^{-7}$ )
Do2011-	13.5	4.4	5800	$1 \times 10^{-2}$	0.58	11.3 ( $2.8 \times 10^{-7}$ )
Gi2012f	13.9	5.6	5603	$1 \times 10^{-2}$	0.58	10.1 ( $2.6 \times 10^{-7}$ )
Fr2008	18.3	6.8	5000	$9 \times 10^{-5}$	0.59	8.4 ( $2.4 \times 10^{-7}$ )
SL2021	19.1	6.9	5200	$4 \times 10^{-5}$	0.59	8.4 ( $2.4 \times 10^{-7}$ )
Do2011	19.2	6.1	4600	$3 \times 10^{-5}$	0.59	9.1 ( $2.5 \times 10^{-7}$ )
Do2011+	27.1	7.8	4000	$7 \times 10^{-9}$	0.59	7.5 ( $2.1 \times 10^{-7}$ )

the spectral energy distribution (SED) shown in Fig. 1. The effect of photon-photon pair-production leads to a noticeable suppression of the apparent brightness at energies exceeding  $\sim 100$  GeV. The observable flux at  $E_\gamma = 18$  TeV is substantially attenuated (in the deep exponential suppression). For the models for the EBL with smaller optical depth [10, 11], the extrapolated and attenuated flux at 18 TeV reaches  $\approx 100$  times the flux of the Crab Nebula. For the model of Ref. [9], the flux at the same energy would be less than  $10^{-4}$  of the Crab Nebula flux.

## 2.2 Expected photon and background counts

In the following, we estimate the number of photons ( $N_\gamma$ ) expected to be detected with LHAASO KM2A within 2000 s after the trigger time. Instead of extrapolating the *Fermi*-LAT flux, we assume that similar to previous GRBs with VHE afterglows, the VHE flux in the afterglow phase is proportional to the soft X-ray flux. This way, we are only left with two unknown parameters, the time of the onset of the afterglow emission (in the following:  $t_1$ ) and the relative normalisation between the X-ray and VHE band ( $\zeta$ ).

Since the afterglows of GRB221009A and GRB190114C share similarities (e.g. the afterglow emission starts a few minutes after the trigger and the observed X-ray light curve follows a power law), we use the time-dependent VHE afterglow spectrum measured with the MAGIC Cherenkov telescopes as a template for GRB221009A [15, 16]. We therefore consider the following assumptions based on observations to estimate the flux and spectral shape for the VHE afterglow of GRB221009A:

1. The VHE-afterglow emission starts at a time  $t_0 + t_1$  after the trigger time  $t_0$  with  $t_1 \approx 10 \text{ s} \dots 200 \text{ s}$ .
2. The ratio  $\zeta = 0.1 \dots 5$  of the VHE energy flux and the soft X-ray energy flux measured remains constant during the afterglow phase.

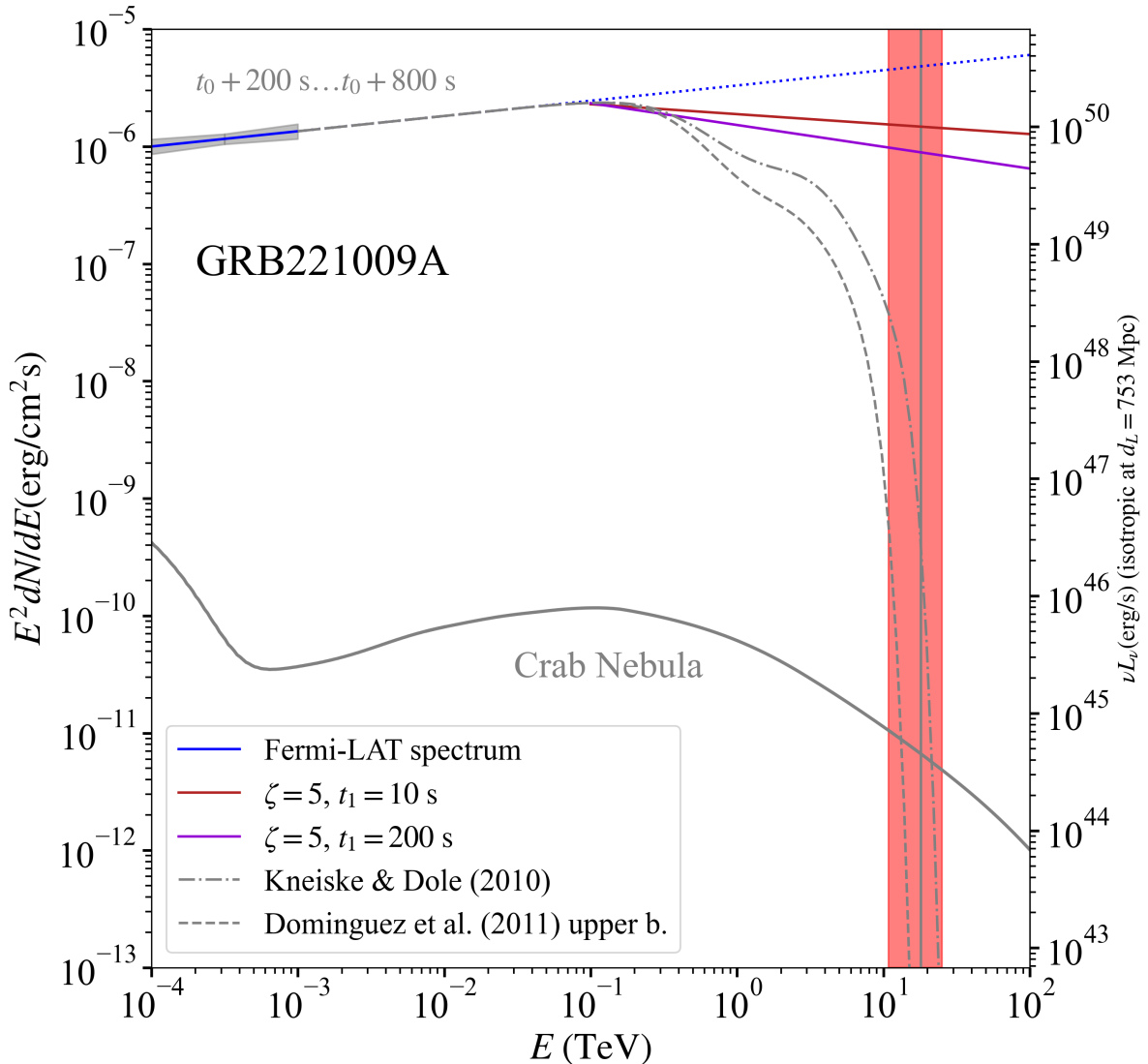


**Figure 1.** Spectral energy distribution (SED) of the high and very high energy emission of GRB221009A. The bow-tie marks the estimated confidence region of the *Fermi*-LAT time averaged spectrum ( $t_0 + 200 \text{ s} \dots t_0 + 800 \text{ s}$ ) and its extrapolation to the highest energies (dotted line). The dash and dash-dotted lines indicate the resulting observable flux when assuming two EBL models which provide the largest and smallest optical depth. For the quantitative analysis, we consider a time-dependent model (see text for details) with two free parameters  $\zeta = F_{VHE}/F_X$  and onset time of the afterglow  $t_1$ . Two exemplary curves are shown in red and magenta. The vertical grey line marks the maximum energy  $E_\gamma$ , while the shaded region indicates the relative energy resolution of 40 %. As a comparison, the SED of the Crab Nebula is overlaid [7].

### 3. The VHE energy spectrum softens during the afterglow.

The second assumption follows from the observation that previous X-ray and VHE-afterglow light curves share a similar power-law behaviour (for GRB180720B see [17] and for GRB190114C see [16]). Observations of GRB221009A with the *Swift*-XRT started about an hour after the trigger and continued up to about a week later. The X-ray afterglow emission  $F_X(t)$  follows a power law in time such that  $F_X(t) \propto t^{-\alpha}$  with  $\alpha = 1.58$  (GCN32802), similar to the value found for GRB190114C.

The VHE energy spectrum of GRB190114C was softening during the first 2000 s such that the photon index after correcting for absorption on the EBL was changing from an initial value of  $\Gamma(t_0 + 100 \text{ s}) \approx -1.9$  to  $\Gamma(t_0 + 2000 \text{ s}) \approx -3$  [16]. The differential flux  $dF = \phi(E, t) dE dt$  for the afterglow starting at  $t_1$  is therefore

$$\phi(E, t) = \phi_0(t) \left(\frac{t}{t_n}\right)^{-\alpha} \left(\frac{E}{E_0}\right)^{-\Gamma(t)}, \quad (2.1)$$

where  $t_n$  is an arbitrary time that determines the normalisation.

We choose  $\phi_0(t)$  such that the energy flux integrated in the VHE band from  $E_1 = 1 \text{ TeV}$  to  $E_2 = 10 \text{ TeV}$

$$F(t) = \int_{E_1}^{E_2} dE E \phi(E, t) \quad (2.2)$$

follows a power law in time

$$F(t) = F_0 \left(\frac{t}{t_n}\right)^{-\alpha}, \quad (2.3)$$

with  $\alpha = 1.5$ , similar to the XRT light curve and  $F_0$  chosen such that for all times  $t > t_1$

$$F(t) = \zeta F_X(t), \quad (2.4)$$

where  $F_X$  is the energy flux in the XRT band. The relative normalisation  $\zeta$  has been found to be close to unity in previous observations. The value of  $\zeta$  is linked to the Comptonization parameter  $Y$  often used in the context of Synchrotron Self-Compton models (see e.g. [18]), where naturally values close to unity are expected. We explore the range from  $\zeta = 0.1$  to  $\zeta = 5$  (see also Fig. 1 where the VHE flux for  $\zeta = 5$  is shown).

The photon index  $\Gamma(t)$  and its dependence on time is parameterised with

$$\Gamma(t) = \Gamma_0 + a \log(t/t_n), \quad (2.5)$$

where  $\Gamma_0 = 1.5$  and  $a = 0.44$  for  $t_n = 200 \text{ s}$  are chosen to match the measured VHE spectrum of the afterglow from GRB190114C [15]. The gradual softening of the spectrum from  $\Gamma = 1.5$  to  $\Gamma \approx 3$  after about one hour of afterglow evolution corresponds to a shift of the peak in the spectral energy distribution from beyond 10 TeV to less than 1 TeV during the observation time. The softening of the VHE spectrum has not been observed for GRB180720B [17] and GRB190829A [19] which were however observed at a later phase of the afterglow.

Any observation of the energy spectrum from a GRB will necessarily be an average of  $\phi(E, t)$  over time<sup>5</sup>. Therefore, we consider the time-average differential spectrum:

$$\phi(E) = \exp(\langle \log \phi_0(t) \rangle - \alpha \langle \log(t/t_n) \rangle) \left(\frac{E}{E_0}\right)^{-\langle \Gamma \rangle}, \quad (2.6)$$

---

<sup>5</sup>Since we require the time-average spectrum to be a power law, we actually average  $\langle \log \phi \rangle_t$

and

$$\langle \Gamma \rangle = \Gamma_0 + a \langle \log(t/t_n) \rangle. \quad (2.7)$$

The time average of  $\log(t/t_n)$  between  $t_1$  and  $t_1 + \Delta t$  is given by

$$\langle \log(t/t_n) \rangle = \frac{t_1}{\Delta t} \log \left( 1 + \frac{\Delta t}{t_1} \right) + \log \left( \frac{t_1 + \Delta t}{t_n} \right) - 1. \quad (2.8)$$

With  $F_0 = \zeta F_X(t = t_n)$  we can re-write

$$\phi_0(t) = \zeta \frac{F_X(t)}{E_0^2 \int dx x^{1-\Gamma(t)}}, \quad (2.9)$$

where the integration is carried out in the interval from  $x = E_1/E_0$  to  $x = E_2/E_0$ .

For  $t_n = 200$  s, we find from the fit to the *Swift*-XRT light curve  $F_X(t_n) \approx 6 \times 10^{-6}$  ergs cm $^{-2}$  s $^{-1}$  (GCN32802).

The time-averaged energy spectrum (assuming no emission for  $t < t_1$ ) in the LHAASO energy range is shown in Fig. 1 for  $\zeta = 5$  and for two different values of  $t_1$ . With a given collection area  $A(E)$ , observation time  $\Delta t$ , and the time-averaged photon flux  $\phi(E)$ , we calculate the expected number of photons  $N_\gamma$  in the energy interval from  $[E_\gamma, 80 \text{ TeV}]$ :

$$N_\gamma(> E_\gamma) = \Delta t \int_{E_\gamma}^{80 \text{ TeV}} \phi(E) A(E) e^{-\tau(E)} dE. \quad (2.10)$$

Even though we are primarily interested to obtain an estimate of the photon number expected above 18 TeV with the KM2A, we nevertheless calculate for consistency the number of photons detectable at lower energy with the WCDA of LHAASO.

The collection area for the WCDA has been released by the LHAASO collaboration as supplementary information.<sup>6</sup> The collection area for the KM2A has been taken from Fig. 2 from [6]. Even though these estimates may not be directly applicable to the particular configuration, event selection cuts, and analysis methods underlying the preliminary LHAASO results, it should be sufficient to get a useful estimate for the KM2A detector<sup>7</sup>. The resulting values for  $N_{\gamma,0.5}$  and  $N_{\gamma,18}$  are listed in Table 2.1 and confirm that the assumptions are reasonable as the event numbers for the WCDA are roughly reproduced. While the values of  $N_{\gamma,0.5}$  do not vary between the different EBL models, the differences between the values found for  $N_{\gamma,18}$  are considerable between  $\approx 10^{-8} \dots 1$ .

The expected number of background events  $N_{\text{cr}}$  of misidentified charged cosmic-ray air showers depends upon the choice of event selection cuts. The background rate  $R_{\text{cr}}$  at 18 TeV for the full KM2A array can be read off Fig. 2 from [20] to be  $R_{\text{cr}} \approx 5$  events/hour. Consequently, the expected number of misidentified events for the  $\Delta t = 2000$  s exposure during the activity of GRB221009A results in  $N_{\text{cr}} \approx 2.8$ .

<sup>6</sup>[http://english.ihep.cas.cn/lhaaso/pdl/202110/t20211026\\_286779.html](http://english.ihep.cas.cn/lhaaso/pdl/202110/t20211026_286779.html)

<sup>7</sup>We note that the WCDA area given in Ref.[6] is roughly 50 times larger at  $E = 1$  TeV than the one presented as supplementary information and used here, while the KM2A areas compare in a consistent way between the two references

### 2.3 Reducing the gamma-ray opacity with Physics beyond the Standard Model

The high optical depth values for some of the considered EBL models reported in Tab. 2.1 suggest that the observation of gamma rays above energies of tens of TeV for the reported GRB redshift is in these cases very unlikely. If the LHAASO event turns out to originate from GRB221009A at an energy of 18 TeV, the effective opacity could be lowered by either the oscillation between photons and hypothetical light pseudo-scalar bosons or by Lorentz Invariance Violation (LIV). We discuss these two scenarios in the following.

#### 2.3.1 Photon mixing with light pseudo-scalar (axion-like) particle

Light pseudo-scalar bosons, often referred to as axions or axion-like particles (ALPs), are predicted in numerous extensions of the Standard Model [see, e.g., 21, for a review] and are plausible candidates for cold dark matter [22–25]. Photons and ALPs could convert into each other in the presence of external magnetic fields. The oscillation would lead to a reduction of the opacity as these particles do not undergo pair-production with background photons.

This process has been studied extensively in connection with gamma-ray observations of blazars and considering different magnetic fields along the line of sight [see, e.g., 26, for a recent review]. As pointed out recently [4], photon-ALP conversions could also be responsible for the observation of the 18 TeV gamma ray reported by LHAASO. Here, we investigate if photon-ALP oscillations could yield the required boost in photon flux to explain the LHAASO observations considering a range of ALP masses  $m_a$  and photon-ALP couplings  $g_{a\gamma}$ . The boost is defined as the ratio  $P_{\gamma\gamma}/\exp(-\tau)$ , where  $P_{\gamma\gamma}$  is the photon survival probability, i.e., the probability to observe an emitted gamma ray when ALPs are considered. The standard EBL attenuation is given by  $\exp(-\tau)$ .

For the astrophysical magnetic fields, we consider a minimal scenario: we include the magnetic field of the host galaxy as well as the magnetic field of the Milky Way. For the host, we conservatively assume mixing in the regular component of a plausible galactic magnetic field. We take the component transversal to the propagation direction to be  $0.5 \mu\text{G}$  coherent over 10 kpc [e.g., 27]. The magnetic field of the Milky Way is described by the regular component of the model in Ref. [28]. We do not consider mixing in the GRB emission region itself as these parameters are at this stage highly uncertain. Including the mixing in the emission region with the parameters used in Ref. [29] does not change our results.

With these model assumptions, we numerically solve the photon-ALP equations of motion using the transfer-matrix approach implemented in the open-source software package GAMMAALPs [30].<sup>8</sup> An example is shown in Fig. 2 for  $m_a = 10^{-7} \text{ eV}$ ,  $g_{a\gamma} = 2 \times 10^{-11} \text{ GeV}^{-1}$ , and the Do2011 model. Clearly, above  $\sim 10 \text{ TeV}$ , the photon flux is greatly enhanced by photon-ALP conversions.

We now perform the calculation of the boost over a grid of  $m_a$  and  $g_{a\gamma}$  at an energy of  $E_\gamma = 18 \text{ TeV}$  to identify the ALP parameter space (given our model assumptions) which could lead to the required boost to explain the LHAASO observation. The result is shown in Fig. 3. Even for comparatively low coupling values above  $2 \times 10^{-12} \text{ GeV}^{-1}$  the boost factor is already a factor of 10 for  $m_a \lesssim 2 \times 10^{-7} \text{ eV}$ .

The values for  $g_{a\gamma}$  listed in Tab. 2.1 are estimated by carrying out the integration in Eqn. 2.10 for  $\zeta = 5$  and  $t_1 = 200 \text{ s}$  after replacing the optical depth  $\tau$  with an effective optical depth  $\tau_{\text{eff}}$  such that  $\tau_{\text{eff}} = -\log(P_{\gamma\gamma})$ . For a fixed value of  $m_a = 10 \text{ neV}$ , the equation  $N_\gamma(E > 18 \text{ TeV}, g_{a\gamma}) = 1$  is then solved for  $g_{a\gamma}$ .

<sup>8</sup><https://gammaalps.readthedocs.io/>



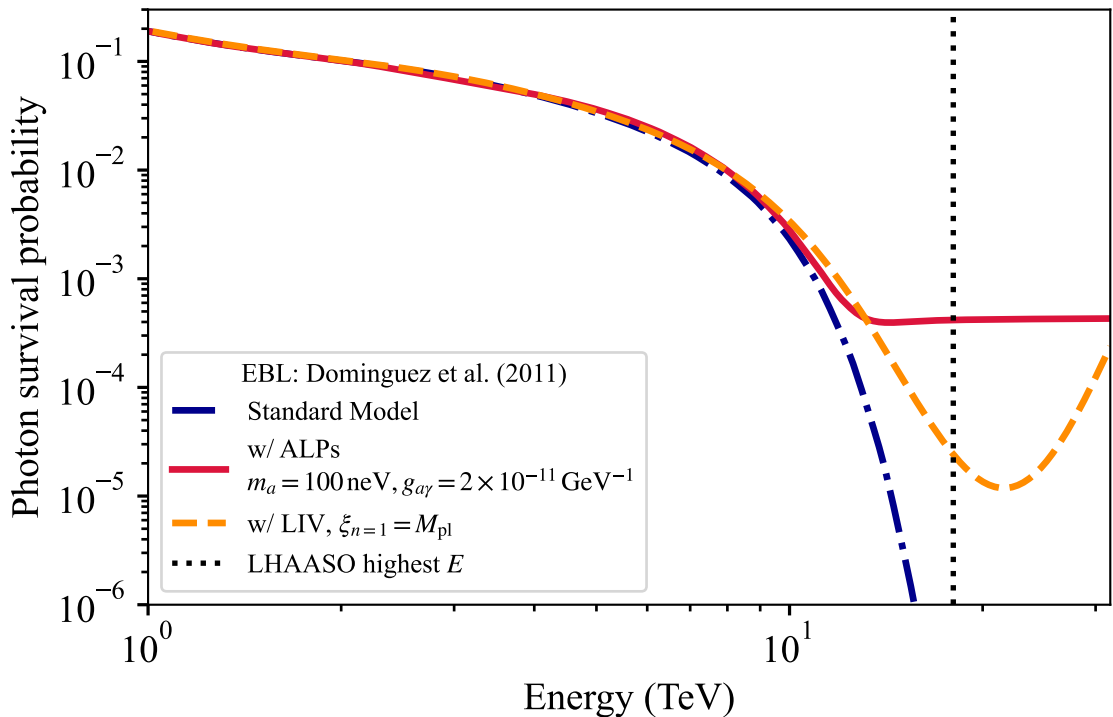


**Figure 2.** An example for the photon survival probability in the presence of ALPs or LIV as a function of energy. ALPs are produced in the host galaxy of the GRB and reconvert into gamma rays in the Galactic magnetic field. For the chosen magnetic field and ALP parameters, this re-conversion leads to an enhanced transparency above  $\sim 10$  TeV. Similarly, the opacity is reduced for the linear LIV effect setting in at energies around the Planck mass  $M_{\text{pl}}$ .

For most considered EBL models, the resulting value for  $g_{a\gamma} \approx 6 \times 10^{-12} \text{ GeV}^{-1}$  is not constrained by the latest bound from the CAST experiment [31] but is in tension with constraints derived from optical polarisation measurements from magnetic white Dwarfs [32] ( $g_{a\gamma} < 5.4 \times 10^{-12} \text{ GeV}^{-1}$  at 90 % c.l.) and from gamma-ray spectra of flat-spectrum radio quasars [7] with  $g_{a\gamma} < 5 \times 10^{-12} \text{ GeV}^{-1}$  (95 % c.l.).

In Fig. 4, we compare the favoured range of values of coupling  $g_{a\gamma}$  for two representative EBL models with the existing bounds mentioned above. For the EBL model with a comparably low optical depth  $\tau_{18} \approx 10$ , there is no need to invoke any photon-ALPs mixing for values of  $\zeta \gtrsim 2.5$ . For models with larger optical depth  $\tau_{18} \approx 20$ , the required value for  $g_{a\gamma}$  exceed the bounds mentioned above unless  $\zeta \gtrsim 5$ . If GRB221009A behaves similarly to previous GRBs with VHE-afterglow emission, the typical value of  $\zeta \approx 1$  would require coupling values for all considered EBL models that are in tension with existing bounds.

A consistent scenario with  $\zeta \approx 1$  and couplings smaller than the upper bounds for  $g_{a\gamma}$  is achievable only for efficient photon-ALPs mixing in the source. At this point, we can not exclude such a scenario. In order to explore the resulting parameters, we assume for simplicity full mixing in the source with subsequent absorption by the EBL such that a pure ALPs beam is re-converted into photons in the magnetic field of the Milky Way. The resulting range of couplings required is indicated as a blue band in Fig. 4. It is comforting to see that both requirements on  $\zeta \approx 1$  and  $g_{a\gamma} < 5 \times 10^{-12} \text{ GeV}^{-1}$  can be fulfilled simultaneously.

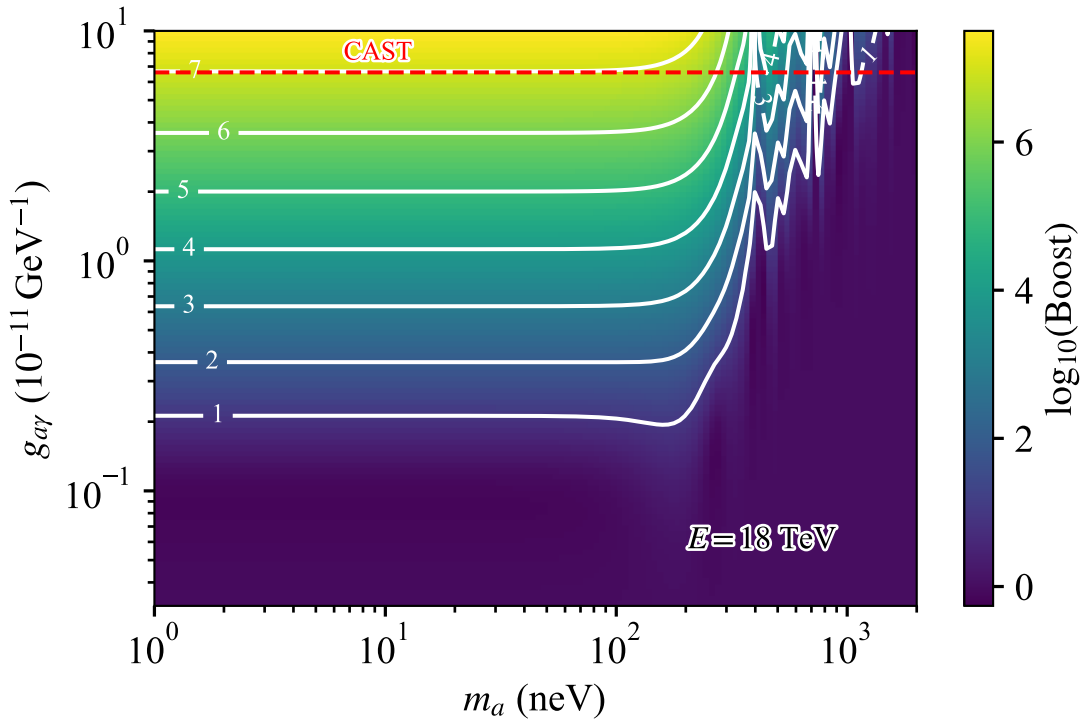


**Figure 3.** The logarithm of the boost factor of the photon flux over a grid of ALP parameters at  $E_\gamma = 18$  TeV. The Do2011 EBL model is assumed. Parameters above the red dashed line are excluded by CAST.

### 2.3.2 Photon opacity in LIV scenarios

Theories of quantum gravity commonly predict LIV [see, e.g., 33] which would have numerous implications for astrophysical observations [e.g., 34, for a review]. Here, we largely follow the reviews in Refs. [26, 34]. Most importantly in the present context, certain effective field theories predict a modified dispersion relation for photons (and electrons) to leading order  $n$ . In the sub-luminal case, the photon velocity (which now depends on the photon energy) is smaller than the speed of light,  $c$ . In this case, the modified dispersion relation leads to a modification of the pair production threshold. For gamma rays of energy  $E_\gamma$  and background photons of energy  $\epsilon$  it now reads,

$$E'_\gamma \epsilon' \geq \frac{2(m_e c^2)^2}{1 - \cos \theta'} + |\xi_n| \frac{E_\gamma^{n+2}}{4M^n}, \quad (2.11)$$

where  $m_e$  is the mass of the electron and  $\theta$  is the angle between the photon momenta.

The primed quantities indicate the comoving frame. The second term in this equation stems from the modified dispersion relation, where  $\xi_n = 1$  if only photons are affected by LIV and  $\xi_n = (1 + 2^{-n})^{-1}$  if both electrons and photons are affected. The energy scale where LIV becomes important is denoted by  $M_n$  and is often given in units of the Planck mass,  $M_{\text{pl}} = \sqrt{\hbar c^5/G} \sim 1.22 \times 10^{28}$  eV. As a consequence of the modified threshold, pair production will be suppressed above some gamma-ray energy. This is illustrated in Fig. 2 for  $M_1 = M_{\text{pl}}$  for  $n = 1$  and for LIV only affecting photons (which we will assume throughout). Clearly, the

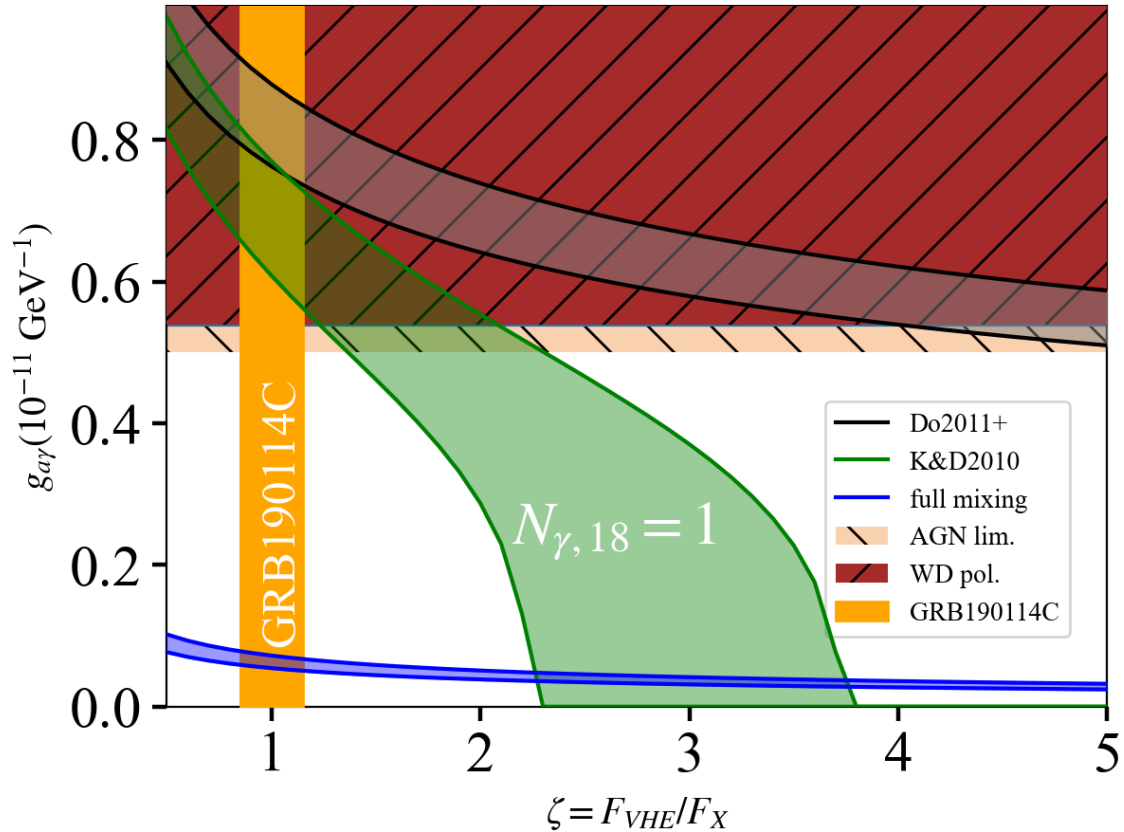


**Figure 4.** Required photon-ALPs coupling  $g_{a\gamma}$  which sufficiently lowers the optical depth for a given EBL model to achieve the number of photons  $N_{\gamma,18} = 1$  as a function of  $\zeta$ . Two separate EBL models are considered which mark the extreme values of optical depth (DOM2011+ and K&D2010 EBL, see also Table 2.1 for more details). For any fixed value of  $\zeta$ , the resulting band marks the coupling values for which  $N_{\gamma,18}$  is unity. The upper and lower bounds relate to the choice of  $t_1 = 200$  s and  $t_1 = 10$  s respectively. The upper bounds on allowed values of  $g_{a\gamma}$  are marked as hatched regions for  $m_a = 10$  neV. The full mixing scenario is independent of the EBL: Here, a maximum mixing in or near the GRB with subsequent complete absorption of photons in the EBL is assumed. The vertical orange region indicates the typical values of  $\zeta$  found in previous GRBs with VHE afterglows.

opacity in the presence of LIV, which we denote with  $\tau_{LIV}$ , is reduced above  $\sim 10$  TeV and the photon survival probability increases towards one above 20 TeV.

We now test for which values of the LIV energy scale  $M$  we achieve a sufficient boost factor  $\exp(-\tau_{LIV} + \tau)$  that would explain the observation of an 18 TeV gamma ray. For both the linear ( $n = 1$ ) and quadratic case ( $n = 2$ ), we step through values of  $M_1$  and  $M_2$  respectively. For each value, we calculate  $\tau_{LIV}$ .<sup>9</sup> The results are shown in Fig. 5. Similar to the case of photon-ALPs mixing, we solve the equation  $N_\gamma(E_\gamma > 18 \text{ TeV}, M_n) = 1$  for  $M_1$  and  $M_2$  separately resulting in the values listed in Tab. 2.1. These values can be considered upper limits for  $M_n$  given that we consider the number of events with energies  $> 18$  TeV<sup>10</sup>.

The favoured parameter space for  $M_1 \lesssim 10^{29}$  eV is in mild tension with searches for a

<sup>9</sup>For this, We use the open-source package EBLTABLE, <https://github.com/me-manu/ebhtable>.

<sup>10</sup>A more detailed consideration of the number of photons reconstructed at  $E_\gamma$  requires detailed knowledge of the energy resolution that is not available to us.

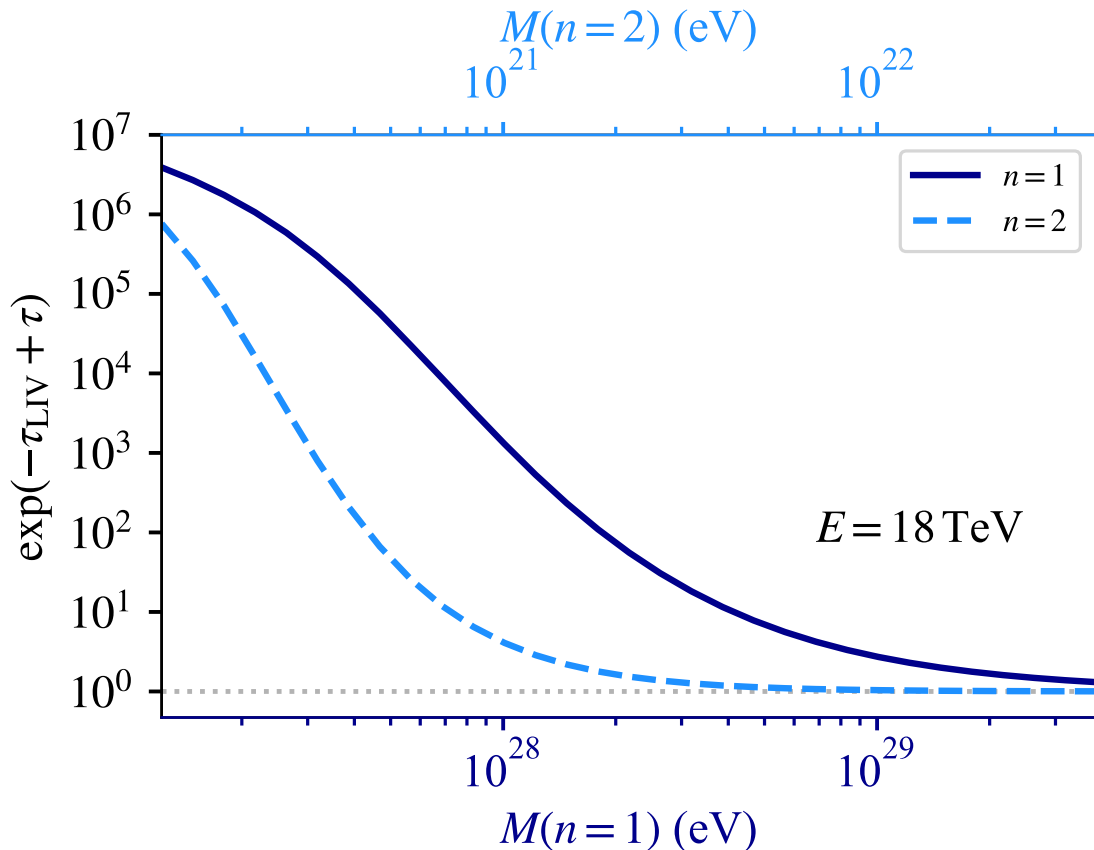


**Figure 5.** The boost factor for LIV of first (lower  $x$  axis) and second order (upper  $x$  axis) as a function of the LIV energy scale at 18 TeV. The Do2011 EBL model is assumed.

reduced opacity using observations of blazars with ground based gamma-ray telescopes. In particular, the stacking of observations of multiple sources constrain  $M_1 \gtrsim 10^{29}$  eV [35].

The situation is more relaxed for EBL models which predict less absorption as can be seen in Fig. 6 (left panel). The green band indicates the region with  $N_{\gamma,18} = 1$  for the EBL model K&D2010 (similar results are obtained for Fi2010). Here, the required values for  $M_1$  even for  $\zeta \approx 1$  are above other constraints. In the case of a predominantly quadratic LIV-breaking scenario ( $n = 2$ ), the optical depth is sufficiently reduced for values of  $M_2 = (2.5 \dots 3.5) \times 10^{21}$  eV which is not excluded by other constraints (see Fig. 6 right panel).

### 3 Conclusions

The ground-based detection of VHE gamma rays from GRB221009A provides an exceptional opportunity to study the acceleration and emission processes. The approximately 5000 photons that are collected above 500 GeV with LHAASO-WCDA from the start of the afterglow up to 2000 s after the trigger are exceptional in comparison to previous VHE afterglow observations: MAGIC detected 877 photons from  $t_0 + 62$  s to  $t_0 + 1227$  s from GRB190114C [15], H.E.S.S. detected 119 photons from GRB180720B during a two-hour observation in the

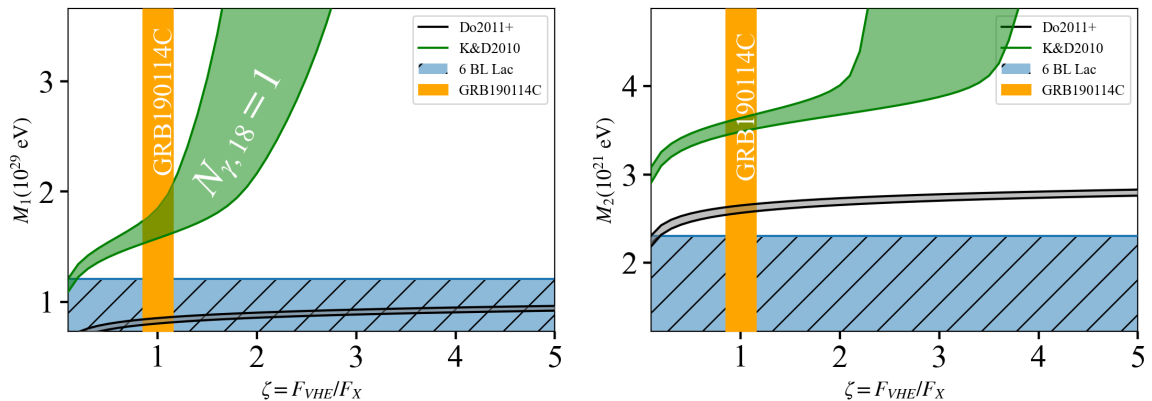


**Figure 6.** Required LIV-breaking energy scale which leads to a reduction of the optical depth such that  $N_{\gamma,18} = 1$ . The left panel shows the resulting favoured region for  $M_1$  in the linear LIV-breaking scenarios ( $n = 1$ ) while the right panel contains the favoured regions for  $M_2$  in the quadratic ( $n = 2$ ) LIV-breaking scenario. In both cases, the favoured range of  $M_{1,2}$  depends on the free parameter  $\zeta = F_{VHE}/F_X$ . The upper and lower bounds of the favoured regions are derived for the onset time  $t_1 = 10$  s and  $t_1 = 200$  s respectively. The blue-hatched region marks the exclusion region obtained from independent observations from gamma-ray spectroscopy.

late phase of the afterglow (10.1 hours after the trigger time). The afterglow emission from GRB190829A was followed even longer: H.E.S.S. carried out follow-up observations between 4 and 56 hours after the trigger time [19]. In all three cases, the VHE afterglows showed a similar temporal behaviour where the VHE flux  $F_{VHE}(t) = \zeta F_X(t)$  with  $\zeta \lesssim 1$ .

In the approach suggested here, we consider the temporal behaviour of the VHE-afterglow emission of GRB221009A to follow the same pattern and choose the *Swift*-XRT light curve of the X-ray afterglow as a proxy to the VHE-afterglow with  $\zeta$  left to vary between 0.1 and 5. In the resulting calculation of event numbers, we can reproduce the number of photons detected above 500 GeV with the WCDA detector of LHAASO under the assumption that  $\zeta \approx 5$ .

The hints for photons detected beyond 10 TeV for GRB221009A ( $z = 0.1505$ ) extend the energy range of photons observed during previous VHE afterglow observations. The origin of the claimed highest energy photon detected with LHAASO (most likely with the KM2A) at  $E_\gamma = 18$  TeV is at first glance difficult to reconcile with the large optical depth at that energy due to pair-production with the extra-galactic background light (EBL).

Among the collection of models for the EBL investigated here (see also Tab. 2.1), the optical depth is expected to be between  $\tau(18 \text{ TeV}) = 9.4 \dots 27.1$ . The probability to detect at least one photon for the extrapolated spectrum calculated with  $\zeta = 5$  could be therefore as small as  $7 \times 10^{-9}$  but reaches values close to unity for other models.

Possible approaches to suppress pair production include photons mixing with light ( $m \lesssim 10^{-7}$  eV) pseudo-scalar particles (such as ALPs) thus avoiding pair production for a small fraction of the photons that re-convert closer to the observer. The resulting values for the mixing  $g_{a\gamma}$  depend on the presence of magnetic fields close to the source. Assuming the EBL model of Ref. [9] and photon-ALP conversions in the hosting galaxies, we find values  $g_{a\gamma} \gtrsim 6 \times 10^{-12} \text{ GeV}^{-1}$  for  $\zeta = 5$  to achieve a sufficiently large boost factor in most of the considered scenarios. The resulting values do not depend very much on the choice of the EBL model as long as the  $\tau_{18} \gtrsim 10$ . The required value for  $g_{a\gamma}$  is in tension with bounds from

other astrophysical observations which constrain  $g_{a\gamma} \lesssim 5 \times 10^{-12} \text{ GeV}^{-1}$ . For values of  $\zeta \approx 1$ , the required photon-ALPs mixing is inconsistent with other bounds. However, a modified scenario with maximum mixing of photon and ALPs near or inside the source would reduce the required  $g_{a\gamma} \lesssim 10^{-12} \text{ GeV}^{-1}$ .

Alternatively, breaking of Lorentz invariance could decrease the gamma-ray opacity. For the quadratic LIV-breaking scenario and  $\zeta \gtrsim 0.1$ , the required values of  $M_2$  are larger than bounds from other observations, independent of the choice of the EBL. In the linear LIV-breaking scenario, only the scenarios with a comparably small optical depth from a lower level of the EBL would not require values of  $M_1$  that are inconsistent with other bounds. It will be interesting to study the arrival time of the TeV photons from GRB221009A to constrain LIV breaking effects independently of the optical depth.

Even if it is exciting to invoke new physics to explain the origin of the photon at 18 TeV, it should be mentioned that the background expectation to detect a mis-identified charged cosmic-ray induced air shower at 18 TeV is consistent with the actual observation.

In conclusion, we have demonstrated that the transparency of the universe could be substantially larger than anticipated for photon-photon pair production if photon-ALP mixing is effective or Lorentz invariance violation occurs at sufficiently low energy scales. Consequently, the observation of bright transients at large optical depth could in principle lead to the discovery of anomalous transparency and provide important clues on the nature of the mechanism for the suppression of pair production.

## Acknowledgments

We acknowledge the support from the Deutsche Forschungsgemeinschaft (DFG, German Research Foundation) under Germany’s Excellence Strategy – EXC 2121 “Quantum Universe” – 390833306. M. M. acknowledges support from the European Research Council (ERC) under the European Union’s Horizon 2020 research and innovation program Grant agreement No. 948689 (AxionDM).

## References

- [1] L. Amati, F. Frontera, M. Tavani, J.J.M. in’t Zand, A. Antonelli, E. Costa et al., *Intrinsic spectra and energetics of BeppoSAX Gamma-Ray Bursts with known redshifts*, *A&A* **390** (2002) 81 [[astro-ph/0205230](#)].
- [2] B. Zhang, *Gamma-ray burst afterglows*, *Advances in Space Research* **40** (2007) 1186 [[astro-ph/0611774](#)].
- [3] J.A. Rueda and R. Ruffini, *On the Induced Gravitational Collapse of a Neutron Star to a Black Hole by a Type Ib/c Supernova*, *ApJ. L.* **758** (2012) L7 [[1206.1684](#)].
- [4] G. Galanti, M. Roncadelli and F. Tavecchio, *Axion-like particles explain the very-high energy emission from GRB221009A*, *arXiv e-prints* (2022) arXiv:2210.05659 [[2210.05659](#)].
- [5] H. Li and B.-Q. Ma, *Lorentz invariance violation induced threshold anomaly versus very-high energy cosmic photon emission from GRB221009A*, *arXiv e-prints* (2022) arXiv:2210.06338 [[2210.06338](#)].
- [6] X.-H. Ma et al., *Chapter 1 LHAASO Instruments and Detector technology \**, *Chin. Phys. C* **46** (2022) 030001.
- [7] L. Dirson and D. Horns, *Phenomenological modelling of the Crab Nebula’s broad-band energy spectrum and its apparent extension*, *arXiv e-prints* (2022) arXiv:2203.11502 [[2203.11502](#)].

- [8] R.J. Gould and G.P. Schröder, *Opacity of the Universe to High-Energy Photons*, *Physical Review* **155** (1967) 1408.
- [9] A. Domínguez, J.R. Primack, D.J. Rosario, F. Prada, R.C. Gilmore, S.M. Faber et al., *Extragalactic background light inferred from AEGIS galaxy-SED-type fractions*, *MNRAS* **410** (2011) 2556 [[1007.1459](#)].
- [10] T.M. Kneiske and H. Dole, *A lower-limit flux for the extragalactic background light*, *A&A* **515** (2010) A19 [[1001.2132](#)].
- [11] J.D. Finke, S. Razzaque and C.D. Dermer, *Modeling the Extragalactic Background Light from Stars and Dust*, *ApJ* **712** (2010) 238 [[0905.1115](#)].
- [12] R.C. Gilmore, R.S. Somerville, J.R. Primack and A. Domínguez, *Semi-analytic modelling of the extragalactic background light and consequences for extragalactic gamma-ray spectra*, *MNRAS* **422** (2012) 3189 [[1104.0671](#)].
- [13] A. Franceschini, G. Rodighiero and M. Vaccari, *Extragalactic optical-infrared background radiation, its time evolution and the cosmic photon-photon opacity*, *A&A* **487** (2008) 837 [[0805.1841](#)].
- [14] A. Saldana-Lopez, A. Domínguez, P.G. Pérez-González, J. Finke, M. Ajello, J.R. Primack et al., *An observational determination of the evolving extragalactic background light from the multiwavelength HST/CANDELS survey in the Fermi and CTA era*, *MNRAS* **507** (2021) 5144 [[2012.03035](#)].
- [15] MAGIC Collaboration, V.A. Acciari, S. Ansoldi, L.A. Antonelli, A. Arbet Engels, D. Baack et al., *Teraelectronvolt emission from the  $\gamma$ -ray burst GRB 190114C*, *Nature* **575** (2019) 455 [[2006.07249](#)].
- [16] MAGIC Collaboration, V.A. Acciari, S. Ansoldi, L.A. Antonelli, A.A. Engels, D. Baack et al., *Observation of inverse Compton emission from a long  $\gamma$ -ray burst*, *Nature* **575** (2019) 459 [[2006.07251](#)].
- [17] H. Abdalla, R. Adam, F. Aharonian, F. Ait Benkhali, E.O. Angüner, M. Arakawa et al., *A very-high-energy component deep in the  $\gamma$ -ray burst afterglow*, *Nature* **575** (2019) 464 [[1911.08961](#)].
- [18] S. Yamasaki and T. Piran, *Analytic modelling of synchrotron self-Compton spectra: Application to GRB 190114C*, *MNRAS* **512** (2022) 2142 [[2112.06945](#)].
- [19] H. E. S. S. Collaboration, H. Abdalla, F. Aharonian, F. Ait Benkhali, E.O. Angüner, C. Arcaro et al., *Revealing x-ray and gamma ray temporal and spectral similarities in the GRB 190829A afterglow*, *Science* **372** (2021) 1081 [[2106.02510](#)].
- [20] Lhaaso Collaboration, Z. Cao, F. Aharonian, Q. An, Axikegu, L.X. Bai et al., *Peta-electron volt gamma-ray emission from the Crab Nebula*, *Science* **373** (2021) 425 [[2111.06545](#)].
- [21] I.G. Irastorza and J. Redondo, *New experimental approaches in the search for axion-like particles*, *Progress in Particle and Nuclear Physics* **102** (2018) 89 [[1801.08127](#)].
- [22] J. Preskill, M.B. Wise and F. Wilczek, *Cosmology of the invisible axion*, *Physics Letters B* **120** (1983) 127.
- [23] L.F. Abbott and P. Sikivie, *A cosmological bound on the invisible axion*, *Physics Letters B* **120** (1983) 133.
- [24] M. Dine and W. Fischler, *The not-so-harmless axion*, *Physics Letters B* **120** (1983) 137.
- [25] P. Arias, D. Cadamuro, M. Goodsell, J. Jaeckel, J. Redondo and A. Ringwald, *WISPy cold dark matter*, *Journal of Cosmology and Astroparticle Physics* **2012** (2012) 013.
- [26] J. Biteau and M. Meyer, *Gamma-Ray Cosmology and Tests of Fundamental Physics*, *Galaxies* **10** (2022) 39 [[2202.00523](#)].

- [27] A. Fletcher, *Magnetic Fields in Nearby Galaxies*, in *The Dynamic Interstellar Medium: A Celebration of the Canadian Galactic Plane Survey*, R. Kothes, T.L. Landecker and A.G. Willis, eds., vol. 438 of *Astronomical Society of the Pacific Conference Series*, p. 197, Dec., 2010 [[1104.2427](#)].
- [28] R. Jansson and G.R. Farrar, *A New Model of the Galactic Magnetic Field*, *ApJ* **757** (2012) 14 [[1204.3662](#)].
- [29] O. Mena, S. Razzaque and F. Villaescusa-Navarro, *Signatures of photon and axion-like particle mixing in the gamma-ray burst jet*, *JCAP* **2011** (2011) 030 [[1101.1903](#)].
- [30] M. Meyer, J. Davies and J. Kuhlmann, *gammaALPs: An open-source python package for computing photon-axion-like-particle oscillations in astrophysical environments*, in *37th International Cosmic Ray Conference*, p. 557, Mar., 2022, DOI [[2108.02061](#)].
- [31] CAST collaboration, *New CAST Limit on the Axion-Photon Interaction*, *Nature Phys.* **13** (2017) 584 [[1705.02290](#)].
- [32] C. Dessert, D. Dunsky and B.R. Safdi, *Upper limit on the axion-photon coupling from magnetic white dwarf polarization*, *PRD* **105** (2022) 103034 [[2203.04319](#)].
- [33] A. Addazi, J. Alvarez-Muniz, R. Alves Batista, G. Amelino-Camelia, V. Antonelli, M. Arzano et al., *Quantum gravity phenomenology at the dawn of the multi-messenger era-A review*, *Progress in Particle and Nuclear Physics* **125** (2022) 103948 [[2111.05659](#)].
- [34] H. Martínez-Huerta, R.G. Lang and V. de Souza, *Lorentz Invariance Violation Tests in Astroparticle Physics*, *Symmetry* **12** (2020) 1232.
- [35] R.G. Lang, H. Martínez-Huerta and V. de Souza, *Improved limits on Lorentz invariance violation from astrophysical gamma-ray sources*, *PRD* **99** (2019) 043015 [[1810.13215](#)].